Structure and Thermal Stability of Bi(III) Oxy-Clusters in Aqueous Solutions

ARTICLE *in* JOURNAL OF SOLUTION CHEMISTRY · FEBRUARY 2014

Impact Factor: 1.18 · DOI: 10.1007/s10953-014-0131-1

7 AUTHORS, INCLUDING:

Joël Brugger
Monash University (Australia)
247 PUBLICATIONS **2,599** CITATIONS
SEE PROFILE

Pascal V. Grundler
Paul Scherrer Institut
31 PUBLICATIONS **300** CITATIONS
SEE PROFILE

J Solution Chem
DOI 10.1007/s10953-014-0131-1

Structure and Thermal Stability of Bi(III) Oxy-Clusters in Aqueous Solutions

Joël Brugger · Blake Tooth · Barbara Etschmann · Weihua Liu · Denis Testemale · Jean-Louis Hazemann · Pascal V. Grundler

Received: 24 May 2013 / Accepted: 9 October 2013

Abstract The structure of Bi(III) clusters in aqueous concentrated acidic perchlorate solutions has been studied by means of X-ray absorption spectroscopy (XAS). The XAS data show that the polynuclear $[Bi_6O_4(OH)_4]^{6+}$ complex with a cage structure predominates at room temperature in acidic Bi-rich solutions. This complex breaks down to form mononuclear complexes with increasing temperature to 428 K. This behavior is consistent with theoretical predictions based on considerations of the electrostatic repulsion, which increases sharply as the dielectric constant of the solvent decreases with increasing temperature.

Keywords Bismuth(III) · Polynuclear complex · X-ray absorption spectroscopy · Ab-initio XANES calculations · Hydrothermal fluids

J. Brugger · B. Tooth · P. V. Grundler
Tectonics, Resources and Exploration (TRaX), School of Earth and Environmental Sciences, University of Adelaide, North Terrace, Adelaide, SA 5005, Australia

J. Brugger · B. Etschmann
South Australian Museum, North Terrace, Adelaide, SA 5000, Australia

Present Address:
J. Brugger (✉)
School of Earth Sciences, Monash University, Clayton, VIC 3168, Australia
e-mail: Joel.Brugger@monash.edu

B. Etschmann
School of Chemical Engineering, University of Adelaide, North Terrace, Adelaide, SA 5005, Australia

W. Liu
CSIRO Earth Science and Resource Engineering, Clayton, VIC 3168, Australia

D. Testemale · J.-L. Hazemann
Institut Néel, Département MCMF, CNRS-Grenoble, 25 Avenue des Martyrs, BP166, 38042 Grenoble Cedex 09, France

Published online: 30 January 2014

Abbreviations

EXAFS	Extended X-ray absorption fine structure
XANES	X-ray absorption near-edge structure
XAS	X-ray absorption spectroscopy

1 Introduction

Aqueous metal-(hydr)oxide clusters (e.g., Lindqvist ion $H_xNb_6O_{19}^{(8-x)-}$) can be used as models for understanding key questions about minerals and their reactions with aqueous solutions (reviewed in [1]). Bismuth(III)-containing nanoclusters also may occur in nature, as suggested for example by the presence of $[Bi_3Fe_7O_6(OH)_2(AsO_4)_9]^{11-}$ anionic nanoclusters in the mineral bouazzerite [2]. Bismuth is a strong Lewis acid and undergoes hydrolysis at low pH values (pH $\leq \sim 1$). The Bi^{3+} aqua ion (i.e. $Bi(H_2O)_n^{3+}$) has been characterized using extended X-ray absorption fine structure (EXAFS) and large angle X-ray scattering (LAXS) in solutions containing 0.662–0.800 mol·L^{-1} Bi(III) and 3.856–5.100 mol·L^{-1} perchlorate by Näslund et al. [3]. This study concluded that eight waters are coordinated to Bi^{3+}. In acidic solutions of pH $\sim$1–3, Bi(III) also forms polynuclear hydrolysis products at moderate bismuth concentrations ($\geq 10^{-2}$ mol·L^{-1} [4, 5]; Fig. 1). Note that Baes and Mesmer [4] excluded $Bi(OH)_2^+$ from their speciation calculations, which led them to overestimate the relative stability of polynuclear species at low Bi(III) concentrations; they depict Bi_6 and Bi_9 species predominating at pH values $\sim$3–7 at a Bi(III) concentration of 10^{-5} mol·L^{-1}, a situation not consistent with experiments [6]. The original estimate of the value of $\log_{10} \beta_2(Bi(OH)_2^+)$ presented by Baes and Mesmer [4] ($\log_{10} \beta_2^\circ = -4.00$) has since been confirmed by new solubility/precipitation [7] and spectrophotometric [8, 9] data.

Polynuclear Bi species containing six and nine Bi(III) ions have been determined by indirect means such as UV–Vis spectrophotometry (10^{-3}–0.01 mol·L^{-1} Bi(III) [10, 11]) and potentiometric titrations (10^{-4}–0.05 mol·L^{-1} [5]). Raman [12] and X-ray scattering [13, 14] experiments, all of which were conducted at very high Bi(III) concentrations ($\geq$4.68 mol·L^{-1} in Bi), confirmed the existence of a polynuclear structure with six Bi atoms in an essentially octahedral arrangement. Originally, the stoichiometry of the Bi_6 cluster was assumed to be $Bi_6(OH)_{12}^{6+}$ [4, 5]; however, identification of the Bi_6 cluster in salts precipitated from Bi-rich acidic solutions [15] led to proposing the $Bi_6O_4(OH)_4^{6+}$ stoichiometry for the cluster in solution. The stoichiometry of the solution species was confirmed to be the same as for the solid by a proton-exchange NMR study conducted in mixed acetone–acid solutions with high Bi(III) concentrations (2.33–2.53 mol·L^{-1} in Bi, 0.45 mol·L^{-1} excess acid [16]). The (Bi_6O_8) cluster is formed by six distorted square pyramidal (BiO_4) units; the edges of the square are shared with the neighboring units (Fig. 1d, f).

This communication reports the X-ray absorption spectroscopic (XAS) characterization of the $Bi_6O_4(OH)_4^{6+}$ cluster in solution and of its thermal stability up to 428 K. We also show that the thermal stability of the $Bi_6O_4(OH)_4^{6+}$ cluster is broadly consistent with the empirical model of Plyasunov and Grenthe [17].

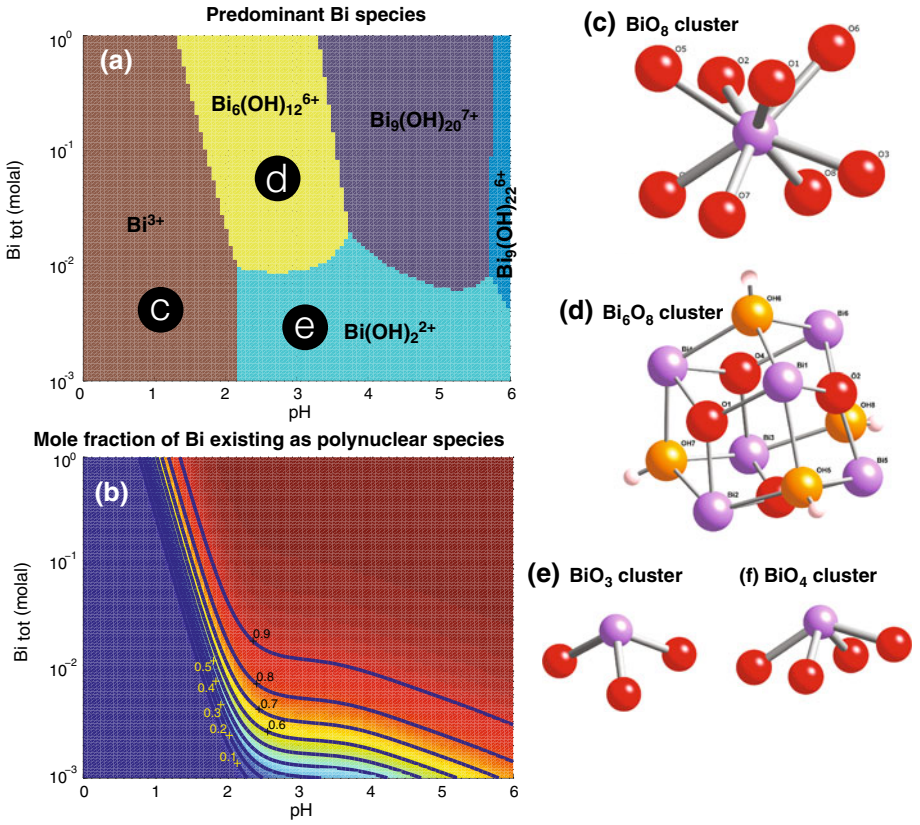

Fig. 1 **a**, **b** Speciation of Bi(III) in acidic solutions. Thermodynamic properties are taken from [4], and equilibrium calculations were performed using Geochemist Workbench [46], for solutions at an ionic strength of $\sim$2.5 mol·kg^{-1}. *Letters* on **a** refer to the structures of the complexes illustrated in (**c**–**e**). **c**–**f** Coordination geometry of Bi(III) complexes: **c** (BiO_8) cluster in the crystal structure of octakis(dimethylsufoxide)bismuth(III) perchlorate [3]; **d** $Bi_6O_4(OH)_4^{6+}$ cluster in the crystal structure of TPH [32] where the cage complex consists of six edge-sharing (BiO_3) pyramids; **e** (BiO_3) cluster, where the trigonal pyramidal coordination is indicative of a stereochemically active lone electron pair; **f** (BiO_4) moiety in the crystal structure of $CaBiO_2Cl_{(s)}$ [35]

2 Materials and Methods

2.1 Materials and Solution Measured

Bismuth oxide in powder form was obtained from Strem Chemicals 'PURATREM' (99.9998 %). Sodium perchlorate solutions were prepared using the monohydrate salt (Aldrich, 99.9 %). Water used in the experiments was obtained from a Millipore direct-Q filtration unit (18.2 MΩ). The sample solution consisted of a perchloric acid solution prepared with $Bi_2O_{3(s)}$, but saturated with respect to $BiOClO_{4(s)}$ (0.14 mol·kg^{-1} perchloric acid, $\sim$0.1 mol·kg^{-1} Bi). Sufficient $Bi_2O_{3(s)}$ was added to have a slight excess of $HClO_4$ on complete dissolution. After overnight dissolution, sonication and gentle heating, the solution still contained a white precipitate that was identified as $BiOClO_{4(s)}$ with a minor

amount of $Bi_{24}ClO_{31(s)}$ by powder X-ray diffraction. The solution was filtered using a 0.25 μm syringe filter prior to measurements. Measurements were conducted from 298 to 423 K at a pressure of 64.5 bar.

2.2 XAS Experiments

Bismuth L_{III} edge (13,419 eV) XAS measurements were performed at BM30B (French Absorption Beamline in Material and Environmental Science, FAME [18, 19]) at the European Synchrotron Radiation Facility (ESRF), Grenoble, France. The X-ray beam energy was calibrated by measuring the Pb L_{III} edge from a 12.5 μm thick reference Pb foil and setting the position of the maximum in the first derivative at 13,053 eV. The Bi L_{III}-edge XAS data were collected over an energy range from 150 eV before the edge to 800 eV after the edge. The measurements were conducted using the hydrothermal spectroscopic autoclave developed by Testemale et al. [20], following the method described by Tooth et al. [21]. The temperature of the fluid at the beam location was calibrated using measurements of the density of water as a function of temperature [22–24], based on the equation of state of pure water (NIST database [25]) and the X-ray mass attenuation coefficients tabulated by Chantler [26]. The Bi(III) concentration was sufficiently large (approximately 0.1 mol·kg^{-1}) that only transmission data were used: 2–4 scans were sufficient to obtain EXAFS spectra exploitable to 12.9 Å^{-1}. The incident (I_o) and transmitted (I_1) intensities were measured by Si photodiodes collecting the X-rays scattered by air. The double crystal Si(220) monochromator provides an energy resolution of 0.67 eV (i.e., ($\Delta E/E$) of 5×10^{-5}) at the Bi-L_{III} edge.

2.3 EXAFS Data Analysis

Data analysis was performed with the HORAE package [27] with FEFF version 9 [28–30]. The k^n-weighted data ($n = 1, 2, 3$) used in the fit ranged from 2.0 to 10–12.9 Å^{-1}, depending on data quality (Table 1). The fitting was done in R-space over the range 1 to 4.2 Å. The identity of the backscattering atoms, Bi-neighbor distance (R), coordination number ($C.N.$), and the Debye–Waller factor (σ^2) for each scattering path retrieved from the R-space fits are presented in Table 1. The influence of anharmonic disorder in determining structural parameters was checked using the cumulant expansion method [31]. The value of the third cumulant ($c3$), found when fitting the Bi first coordination shell, always converged to zero within error ($\pm 10^{-3}$). The presence of multiple scattering (MS) events within the Bi first coordination shell was also tested using the FEFF code, assuming geometries around Bi(III) as found in the model compounds investigated. The MS contributions in the experimental EXAFS spectra of the studied systems were found to be negligible.

2.4 Ab-initio XANES Calculations

The XANES spectra for the $Bi_6O_4(OH)_4^{6+}$ cluster found in the crystal structure of tetra-oxotetrahydroxohexabismuth(III) perchlorate heptahydrate (TPH) [32] were calculated ab initio using the FDMNES package [33], following the procedure outlined in our earlier studies [21–23, 34]. In addition, calculations were conducted for the $CaBiO_2Cl(s)$ compound, based on the crystal structure of Fray et al. [35], and for the Bi^{3+} aqua ion, based on the (BiO_8) moiety found in octakis(dimethylsufoxide)bismuth(III) perchlorate [3]. The atoms were kept neutral for all of the calculations [36, 37]. The raw calculations represent

Table 1 Results of EXAFS data analysis

Experiment	Temperature and pressure	[Bi] (molal)	k-range (Å^{-1})	R-range (Å)	Scattering atom	C.N.	R (Å)	σ^2 (Å ^{2})	ΔE_0 (eV)	χ^2_{red}	R
Exp7/Poly Fit1	298 K 1 bar	0.1	2–12.9	1–4.2	O1	1 (fix)	Bi–O1 = 2.13(9)	0.0028(5)	−2(1)	82	0.023
					O2	1 (fix)	Bi–O2 = 2.20(8)	0.0028(5)[a]			
					O3	1 (fix)	Bi–O3 = 2.24(3)	0.019(6)			
					O4	1 (fix)	Bi–O4 = 2.58(5)	0.019(6)[a]			
					O5	1 (fix)	Bi–O5 = 2.68(2)	0.07[d]			
					O6	1 (fix)	Bi–O6 = 2.77(2)	0.07[d]			
					O7	1 (fix)	Bi–O7 = 3.1910	0.005(3)			
					O8	1 (fix)	Bi–O8 = 3.3582	0.005(3)[a]			
					O9	1 (fix)	Bi–O9 = 3.4944	0.0028(5)[a]			
					Bi1	1 (fix)	Bi–Bi1 = 3.63(3)	0.003(2)			
					Bi2	1 (fix)	Bi–Bi2 = 3.64(3)	0.003(2)[a]			
					Bi3	1 (fix)	Bi–Bi3 = 3.75(3)	0.003(1)			
					Bi4	1 (fix)	Bi–Bi4 = 3.76(3)	0.003(1)[a]			
					Cl	1 (fix)	Bi–Cl = 4.03(7)	0.011(5)			
Exp7/Poly Fit2	298 K 1 bar	0.1	2–12.9	1–4.2	O1	1 (fix)	Bi–O1 = 2.13(9)	0.0028(5)	−2(1)	74	0.018
					O2	1 (fix)	Bi–O2 = 2.20(8)	0.0028(5)[a]			
					O7	1 (fix)	Bi–O7 = 3.1910	0.005(3)			
					O8	1 (fix)	Bi–O8 = 3.3582	0.005(3)[a]			
					O9	1 (fix)	Bi–O9 = 3.4944	0.0028(5)[a]			
					Bi1	1 (fix)	Bi–Bi1 = 3.63(3)	0.003(2)			
					Bi2	1 (fix)	Bi–Bi2 = 3.64(3)	0.003(2)[a]			
					Bi3	1 (fix)	Bi–Bi3 = 3.75(3)	0.003(1)			
					Bi4	1 (fix)	Bi–Bi4 = 3.76(3)	0.003(1)[a]			
					Cl	1 (fix)	Bi–Cl = 4.03(7)	0.011(5)			

Table 1 continued

Experiment	Temperature and pressure	[Bi] (molal)	k-range (Å^{-1})	R-range (Å)	Scattering atom	C.N.	R (Å)	σ^2 (Å ^{2})	ΔE_0 (eV)	χ^2_{red}	R
Exp7/Poly Fit3	298 K 1 bar	0.1	2–12.9	1–4.2	O1	1.5(1)	Bi–O1 = 2.167(8)	0.002(1)	0(1)	217	0.033
					Bi2	4 (fix)	Bi–Bi2 = 3.69(2)	0.009(2)			
					Cl	1 (fix)	Bi–Cl = 4.15(8)	0.01(1)			
Exp7/Poly[c] FitA	428 K 64.5 bar	0.1	2–12.9	1–4.2	O1	1 (fix) × 0.8(3)	Bi–O1 = 2.13[b]	0.004(5)	1.3(4)	53	0.03
					O2	1 (fix) × 0.8(3)	Bi–O2 = 2.21[b]	0.004(5)[a]			
					O7	1 (fix) × 0.8(3)	Bi–O7 = 2.75(4)	0.003			
					O8	1 (fix) × 0.8(3)	Bi–O8 = 3.04[b]	0.003			
					O9	1 (fix) × 0.8(3)	Bi–O9 = 3.31[b]	0.003			
					Bi1	1 (fix) × 0.8(3)	Bi–Bi1 = 3.67[b]	0.009(5)			
					Bi2	1 (fix) × 0.8(3)	Bi–Bi2 = 3.713[b]	0.009(5)[a]			
					Bi3	1 (fix) × 0.8(3)	Bi–Bi3 = 3.75(13)	0.009(5)[a]			
					Bi4	1 (fix) × 0.8(3)	Bi–Bi4 = 3.72[b]	0.009(5)[a]			
					Cl	1 (fix) × 0.8(3)	Bi–Cl = 3.72[b]	0.003			
					O	3 (fix) × 0.2(3)	Bi–O = 2.13(7)	0.003			

k, k^2, k^3 weighted EXAFS fits for 298 data, but only k^2 weighting used for 428 K data

[a] Constrained to be the same as another Debye–Waller factor

[b] These bond lengths were fixed in the fit

[c] Modeled as a mixture of $[Bi_6O_8]$ and $[BiO_3]$

[d] A small value of σ^2 increases χ^2; e.g. for $\sigma^2 = 0.019$, $\chi^2 = 252$

the photo-absorption cross-section, related to the transition amplitudes between initial and final states. To make these calculated spectra comparable with experimental spectra, the raw calculations were convoluted with a Lorentzian function that has an energy-dependent width in order to reproduce the core–hole lifetime broadening (6.00 eV for the Bi L_{III} edge [38]) and the inelastic plasmon interactions with the photoelectron, and with a Gaussian function to reproduce the experimental resolution, 0.67 eV in this case [18, 19]. A further convolution parameter in FDMNES is the Fermi energy (E_{Fermi}); the states beneath the Fermi level are occupied, and thus the cross section is set to zero. A value of 9.6 eV was chosen by trial and error as it produced a closer agreement for the shape of the white line.

3 The $Bi_6O_4(OH)^{6+}_{4\,(aq)}$ Cluster

The Fourier transform of the 298 K solution data confirms the predominance of polynuclear species in this solution, as indicated by a strong peak corresponding to the expected Bi–Bi distances in the R-space plot (Fig. 2a). This dataset could be fitted well with the $Bi_6O_4(OH)^{6+}_4$ complex, using the cluster found in the crystal structure of TPH as a model [15, 32] (Table 1). The $Bi_6O_4(OH)^{6+}_4$ cluster in TPH shows significant distortion. The six Bi atoms sit on independent crystallographic sites, and are surrounded by two oxygens with Bi–O distances at 2.13–2.23 Å and two hydroxide groups with Bi–O distances at 2.32–2.51 Å, resulting in a distorted BiO_{2+2} first shell coordination (Fig. 1d, f). Each Bi atom is surrounded by four Bi atoms belonging to the same cluster at a distance of 3.65–3.78 Å. In addition to contributions from the atoms within the $Bi_6O_4(OH)^{6+}_4$ cluster, the Bi atoms in TPH are coordinated by water molecules (2/3 H_2O on average at a distance up to 2.9 Å) and 3.5 chloride atoms from perchlorate groups at Bi–Cl distances of 3.62–4.45 Å.

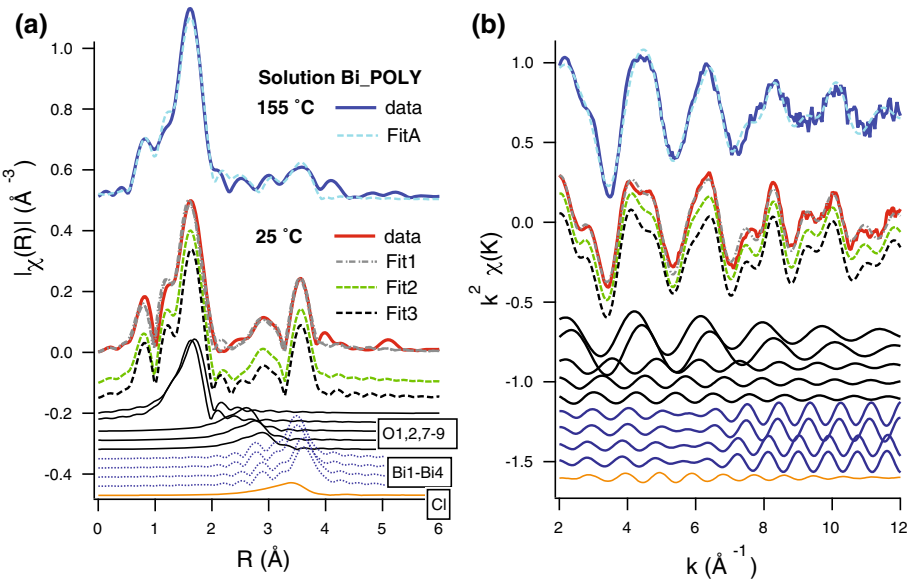

Fig. 2 EXAFS data and refinements for the Bi_POLY experiments

The R-space data for the room-temperature Bi_POLY solution shows a clear peak at ~3.7 Å (Fig. 2a), which can be fitted with four Bi at distances of 3.63–3.76 Å, similar to the Bi–Bi distances in the TPH $Bi_6O_4(OH)_4^{6+}$ cluster. LAXS revealed average Bi–Bi distances of ~3.69 Å for Bi(III) in concentrated perchlorate solutions, in agreement with our EXAFS analysis [3, 13, 14]. The presence of four Bi–Bi interactions at ~3.7 Å is a strong indication that a cluster such as $Bi_6O_4(OH)_4^{6+}$ is the dominant form of Bi(III) in solution. To further test this hypothesis, we present a model based on a total of 14 paths (labeled as Fit1 in Fig. 2 and Table 1). This model shows a good agreement with the $Bi_6O_4(OH)_4^{6+}$ cluster in TPH, with totals of two oxygens at Bi–O < 2.0 Å, and nine oxygens at <3.6 Å (average of 8.67 O in the crystal structure). Overall, these results are consistent with the existence of the $Bi_6O_4(OH)_4^{6+}$ cluster in solution, and suggest that this cluster itself is coordinated by perchlorates and water molecules. However, the complexity of the structure of the $Bi_6O_4(OH)_4^{6+}$ cluster renders quantitative interpretation of the EXAFS data for O delicate. For example, the O atoms at ~2.5 Å (corresponding to Bi–OH bonds in TPH) have a near-negligible effect on the fit. Observation of the individual scattering paths shown in Fig. 2b reveals that destructive wave interferences give rise to the obscuring of this feature in the resulting spectra. Indeed, only a small peak at ~2.5 Å is evident in the R-space plot and the inclusion of extra scattering paths results in a slightly better fit (no statistically significant improvement). A simplified model using only ten paths (excluding the oxygen atoms at ~2.5 Å) resulted in an almost equally good fit (labeled as Fit2 in Fig. 2). An even simpler model, using only three paths gave an almost equally good fit visually (labeled as Fit3 in Fig. 2), but was statistically significantly worse than Fit1 and Fit2 (Table 1). The EXAFS distance for Bi–O is consistent with values found in solids and in LAXS solution studies [3, 14]. The range of distances obtained for the coordinated oxygens at higher distance correspond to hydroxides, but also to coordination with water and perchlorate in the solvent.

The results of the XANES calculations are shown in Fig. 3. The spectra of Ca-BiO_2Cl(s) (BiO_4 moiety, Fig. 1f) and Bi^{3+} (BiO_8 moiety, Fig. 1c) are shown to illustrate the change in the XANES spectrum as a function of complex geometry and the level of agreement between calculated and measured spectra. In both cases, the raw spectra show that all the locations and qualitative intensities of the spectral features are accurately reproduced. In general the convoluted spectra also show a good agreement, although the amplitude of some features may be underestimated. Calculations for the $[Bi_6O_4(OH)_4]$ cluster are based on the cluster found in the TPH crystal structure [32]. As the six Bi atoms in the cluster occupy different crystallographic sites, the XANES spectrum for this cluster is the average of six individual calculations, each conducted to a radius of 4 Å; the individual raw calculations are shown in Fig. 3 together with the convoluted spectra. The position and relative intensity of the spectral features are accurately reproduced. Note that the white line appears broader and has less feature in the experimental spectrum; most likely, this represents a higher level of disorder and/or distortion in the aqueous cluster compared to the calculations based on a single geometry found in a crystal structure.

4 Breakdown of Polynuclear Species at Elevated Temperature

With increasing temperature, the amplitude of the peak corresponding to Bi–Bi interactions in the R-space plots of the data for the Bi_POLY solution decreases, indicating clearly the breakdown of the polynuclear structure upon heating (Fig. 2a). The XANES data collected at 428 K can be fitted as a linear combination of 71 % $Bi_6O_4(OH)_4^{6+}$ (solution Bi_POLY at

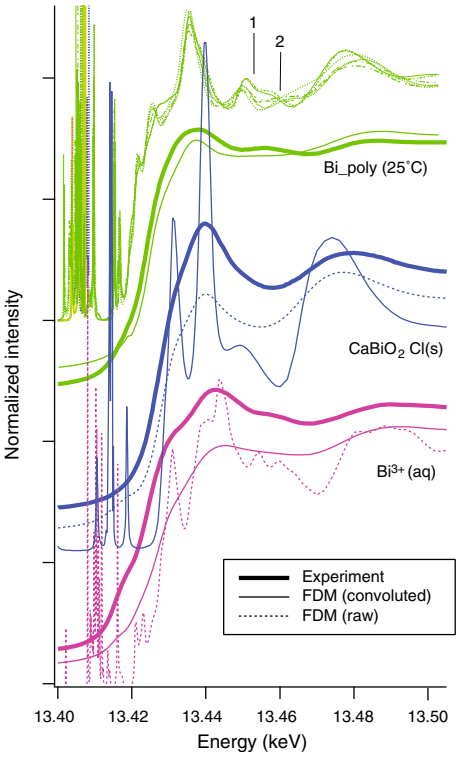

Fig. 3 Ab-initio XANES simulations for solutions containing the polynuclear $Bi_6O_4(OH)_4^{6+}$ complex, based on the crystal structure of TPH [32], compared with the experimental spectrum obtained on the Bi_POLY solution. Calculations were conducted in the FDM mode, for a radius of 4 Å. The figure also shows the experimental (measured in transmission mode) and calculated spectra from $CaBiO_2Cl(s)$ (calculations based on the crystal structure of Fray et al. [35]; calculation radius = 6 Å) and for Bi^{3+} (measurements: solution containing 0.03 mol·kg^{-1} Bi(III) in 3.67 mol·kg^{-1} in $HClO_4$; calculations for the (BiO_8) moiety found in octakis(dimethylsufoxide)bismuth(III) perchlorate [3]

298 K) + 29 % (BiO_3) (corresponding to the aqueous complex $Bi(OH)_3(aq)$; [21]). An equally good fit of the XANES data can be obtained using 50 % of the polynuclear Bi, 35 % BiO_3, and 15 % Bi^{3+}. A careful observation of the Fourier transforms for the different solutions shows that solutions containing the Bi^{3+} aqua ion have a longer average Bi–O bond length (peak at 1.81 Å, un-phase-shifted; [3]) than either the polynuclear Bi complex at 298 K (1.66 Å) or 428 K (1.63 Å) (Fig. 2a), or the $Bi(OH)_3(aq)$ complex (1.53–1.60 Å [21]); this strongly suggests that the breakdown products of the $Bi_6O_4(OH)_4^{6+}$ complex retains mainly the (BiO_3) geometry. Thus, based on bond lengths, it is expected that while the (BiO_8) complex may exist in solution, under these conditions the amount would be quite small and the breakdown of the polynuclear species can be explained simply using a linear combination of the 298 K polynuclear data and a species with BiO_3 geometry (e.g., $[Bi(OH)_2{\cdot}H_2O)]^+$ [21]; Fig. 1). This is consistent with the EXAFS data for the Bi_POLY solution at 428 K, which can be modeled using a mixture of Bi_6O_8 (based on the 298 K fit) and BiO_3 (Fit A, Table 1).

The breakdown of the polynuclear $Bi_6O_4(OH)_4^{6+}$ species is consistent with the predictions concerning the temperature dependence of equilibria between polynuclear and mononuclear

species. Plyasunov and Grethe [17] tested and applied a semi-empirical model for estimating the temperature dependence of the formation of cationic polynuclear complexes based on a simple electrostatic model. This model had originally been proposed by Gurney [39] and modified by Ryzhenko [40] and Bryzgalin and Rafal'sky [41]. For the reaction

$$6Bi^{3+} + \ 12OH^- \rightleftharpoons Bi_6O_4(OH)_4^{6+} + 4H_2O \tag{1}$$

$$\log_{10}K(T,p) = \frac{298.15}{T}\log_{10}K(298.1\text{K}) + \text{A}\frac{e^2N}{aRT\ln 10}\left(\frac{1}{D(T,p)} - \frac{1}{D(298.1\text{K})}\right), \tag{2}$$

where $\text{A} = u|Z_cZ_a|_{\text{efBi(OH)}_2^+} - \frac{u(u-1)}{8}Z^2_{\text{Bi(OH)}_2^+}$, $|Z_cZ_a|_{\text{efBi(OH)}_2^+} = L|Z_cZ_a| - QZ_a^2 + \frac{\alpha Z_c^2 L}{2a^3} - \frac{(\alpha Z_c)^2 Q}{2a^6}$, e is the charge of the electron, N is Avogadro's number, D is the dielectric constant of water taken from [42], a is an "electrostatic bond" distance for Bi^{3+}–OH^- (see below); a varies with temperature following $a(T,p) = a(298.1\text{K}, 1\text{bar})\left(\frac{V(T,p)}{V(298.1\text{K},1\text{bar})}\right)^{1/3}$, where $V(T, p)$ are the molar volume of pure water, u is a stoichiometric coefficient corresponding to the number of metal ions in the polynuclear complex ($u = 6$), Z_c is the charge of the cation on the left side of Eq. 1 ($Z_c = 3$), Z_a is the charge of the anion on the left side of Eq. 2 ($Z_a = -1$), $|Z_cZ_a|_{\text{efBi(OH)}_2^+}$ is the "effective charge" term for $Bi(OH)_2^+$, L is the number of ligands in $Bi(OH)_2^+$ ($L = 2$), Q is a stereochemical factor depending on L with $Q = (3L^2 - 5L + 2)/8$, and α is the polarizability of the anion, taken to be 2.04×10^{-24} cm^3 for OH^-. For these equations the temperature is in Kelvin.

The distance a can be estimated from measurements of the entropy or Gibbs energy of formation of mononuclear complexes, thus the a parameter can be derived from measurements of the formation constants of $Bi(OH)_2^+$ and $Bi(OH)_3$(aq) [21, 43] by fitting to the following equation for the reactions:

$$Bi^{3+} + L(OH)^- \rightleftharpoons Bi(OH)_L^{3-L}$$

$$\log_{10}K(T,p) = \frac{298.15}{T}\log_{10}K(298.1\text{K}) + \frac{|Z_cZ_a|_{\text{ef}}e^2N}{a(T,p)RT\ln 10}\left(\frac{1}{D(T,p)} - \frac{1}{D(298.1\text{K})}\right) \tag{3}$$

The following values were obtained (95 % confidence level errors) for a(298.1 K, 1 bar): 2.28(33) Å {$Bi(OH)_3$(aq) [43]}; 1.97(4) Å {$Bi(OH)_3$(aq) [21])}; and 2.4(–0.7/ + 0.4) Å {$Bi(OH)_2^+$ [43]}. These a(298.1 K, 1 bar) values span the range between the distance measured by EXAFS for the $Bi(OH)_3$(aq) complex at $T \geq 573$ K (2.08(1) Å), which displays a trigonal pyramidal geometry [21], and the sum of the crystallographic radii of Bi^{3+} in octahedral coordination and O^{2-} (2.43 Å [44]).

Using a(298.1 K, 1 bar) values of 2.0 and 2.4, we calculate that the formation constants for Eq. 1 at 423 K are 157 and 148, respectively, decreasing from 174 at 298 K [5]. Speciation calculations using these values and the extended Debye–Hückel activity coefficient model (b-dot equation [45]) confirm that at room-temperature, >99 mol% of the Bi is present as $Bi_6O_4(OH)_4^{6+}$. The calculation predicts that $Bi_6O_4(OH)_4^{6+}$ is still dominant at 428 K, accounting for >99 and ~91 mol% of the Bi(III) for a(298.1, 1 bar) values of 2.0 and 2.4, respectively. Both this value of 91 mol% Bi and 71 mol% (derived the linear combination fit of the XANES data) agree that most of the Bi(III) in solution is present within the polynuclear species. According to the available thermodynamic properties for Bi(III) hydroxides, the main decomposition product is $Bi(OH)_2^+$, which is also consistent with the observed XANES spectra. The decrease of the relative stability of polynuclear

complexes with increasing temperature is due to the large increase of electrostatic repulsion related to the decrease of the dielectric constant of water [17]. This decrease in thermal stability of the polynuclear complex can be predicted accurately using the model confirmed by Plyasunov and Grenthe [17]; however, the extrapolated $\log_{10} K$ values are highly sensitive to the choice of the a(298.1 K, 1 bar) parameter.

References

1. Spiccia, L., Casey, W.H.: Synthesis of experimental models for molecular inorganic geochemistry—a review with examples. Geochim. Cosmochim. Acta **71**, 5590–5604 (2007)
2. Brugger, J., Meisser, N., Krivovichev, S., Armbruster, T., Favreau, G.: Mineralogy and crystal structure of bouazzerite from Bou Azzer, Anti-Atlas, Morocco: Bi–As–Fe nanoclusters containing Fe^{3+} in trigonal prismatic coordination. Am. Mineral. **92**, 1630–1639 (2007)
3. Näslund, J., Persson, I., Sandström, M.: Solvation of the bismuth(III) ion by water, dimethyl sulfoxide, *N*,*N*′-dimethylpropyleneurea, and *N*,*N*-dimethylthioformamide. An EXAFS, large-angle X-ray scattering, and crystallographic structural study. Inorg. Chem. **39**, 4012–4021 (2000)
4. Baes, C.F., Mesmer, R.E.: The Hydrolysis of Cations. Wiley, New York (1976)
5. Olin, Å.: Studies on the hydrolysis of metal ions 19. The hydrolysis of bismuth(III) in perchlorate medium. Acta Chem. Scand. **11**, 1445–1456 (1957)
6. Bidleman, T.F.: Bismuth–dithizone equilibria and hydrolysis of bismuth ion in aqueous solution. Anal. Chim. Acta **56**, 221–231 (1971)
7. Kragten, J., Decnop-Weever, L.G., Gründler, P.: Mixed hydroxide complex formation and solubility of bismuth in nitrate and perchlorate medium. Talanta **40**, 485–490 (1993)
8. Antonovich, V.P., Nevskaya, E.M., Shelikhina, E.I., Nazarenko, V.A.: Spectrophotometric determination of the hydrolysis constants of monomeric bismuth ions. Zh. Neorg. Khim. **20**, 968–974 (1975)
9. Brachmann, A., Geipel, G., Bernhard, G., Nitsche, H.: UV-Vis spectroscopic study of Bi^{3+} hydrolysis. In: Nitsche, H. (ed.) Annual Report Forschungszentrum Rossendorf, pp. 16–18. Institute of Radiochemistry, Dresden (1994)
10. Dragalescu, C., Nimara, A., Julean, I.: Contributions to the bismuth hydrolysis study I. Spectrophotometric and polarographic investigations on bismuth perchlorate hydrolysis. Chem. Anal. **17**, 631–641 (1972)
11. Dragalescu, C., Nimara, A., Julean, I.: Contributions to the bismuth hydrolysis study II. Spectrophotometric and polarographic investigations on bismuthyl perchlorate hydrolysis. Rev. Rou. Chim. **7**, 1181–1190 (1972)
12. Maroni, V.A., Spiro, T.G.: The vibrational spectrum of the hydrolytic hexamer of bismuth(III). J. Am. Chem. Soc. **88**, 1410–1412 (1965)
13. Levy, H.A., Danford, M.D., Agron, P.A.: X-ray diffraction study of bismuth polymer in aqueous perchlorate solution. J. Chem. Phys. **31**, 1458–1461 (1959)
14. Sundvall, B.: An X-ray diffraction study of the hexanuclear complex of Bi(III) in aqueous perchlorate solution. Determination of the oxygen positions. Acta Chem. Scand. A **34**, 93–98 (1980)
15. Sundvall, B.: On the crystal structure of dodecahydroxohexabismuth(III) perchlorate. Acta Chem. Scand. A **28**, 1036–1041 (1974)
16. Grenthe, I., Toth, I.: 1H NMR studies of the Bi^{3+}–HO^- system: stoichiometric composition of the hexanuclear complex and rate of proton exchange of coordinated H_2O and HO^- in mixed acetone/water solution. Inorg. Chem. **24**, 2405–2407 (1985)
17. Plyasunov, A.V., Grenthe, I.: The temperature dependence of stability constants for the formation of polynuclear complexes. Geochim. Cosmochim. Acta **58**, 3561–3582 (1994)
18. Proux, O., Biquard, X., Lahera, E., Menthonnex, J.J., Prat, A., Ulrich, O., Soldo, Y., Trevisson, P., Kapoujyan, G., Perroux, G., Taunier, P., Grand, D., Jeantet, P., Deleglise, M., Roux, J.P., Hazemann, J.L.: FAME: a new beamline for X-ray absorption investigations of very diluted systems of environmental, material and biological interests. Phys. Scr. **T115**, 970–973 (2005)
19. Proux, O., Nassif, V., Prat, A., Ulrich, O., Lahera, E., Biquard, X., Menthonnex, J.J., Hazemann, J.L.: Feedback system of a liquid-nitrogen-cooled double-crystal monochromator: design and performances. J. Synchrotron Radiat. **13**, 59–68 (2006)
20. Testemale, D., Argoud, R., Geaymond, O., Hazemann, J.L.: High pressure high temperature cell for X-ray absorption and scattering techniques. Rev. Sci. Instrum. **76**, 043905 (2005)

21. Tooth, B., Etschmann, B., Pokrovski, G.S., Testemale, D., Hazemann, J.-L., Grundler, P.V., Brugger, J.: Bismuth speciation in hydrothermal fluids: an X-ray absorption spectroscopy and solubility study. Geochim. Cosmochim. Acta **101**, 156–172 (2013)
22. Brugger, J., Etschmann, B., Liu, W., Testemale, D., Hazemann, J.-L., Emerich, H., van Beek, W., Proux, O.: An XAS study of the chloride complexing of Cu(I) in brines up to high temperature (400 °C, 600 bar). Geochim. Cosmochim. Acta **71**, 4920–4941 (2007)
23. Etschmann, B.E., Liu, W., Testemale, D., Muller, H., Rae, N.A., Proux, O., Hazemann, J.L., Brugger, J.: An in situ XAS study of copper(I) transport as hydrosulfide complexes in hydrothermal solutions (25–592 °C, 180–600 bar): speciation and solubility in vapor and liquid phases. Geochim. Cosmochim. Acta **74**, 4723–4739 (2010)
24. Liu, W.H., Borg, S.J., Testemale, D., Etschmann, B., Hazemann, J.L., Brugger, J.: Speciation and thermodynamic properties for cobalt chloride complexes in hydrothermal fluids at 35–440 °C and 600 bar: an in situ XAS study. Geochim. Cosmochim. Acta **75**, 1227–1248 (2011)
25. Lemmon, E.W., McLinden, M.O., Friend, D.G.: Thermophysical Properties of Fluid Systems. National Institute of Standards and Technology, Gaithersberg (2000)
26. Chantler, C.: Theoretical form factor, attenuation, and scattering tabulation for $Z = 1$–92 from $E = 1$–10 eV to $E = 0.4$–1.0 MeV. J. Phys. Chem. Ref. Data **24**, 71–591 (1995)
27. Ravel, B., Newville, M.: ATHENA, ARTEMIS, HEPHAESTUS: data analysis for X-ray absorption spectroscopy using IFEFFIT. J. Synchrotron Radiat. **12**, 537–541 (2005)
28. Zabinsky, S.I., Rehr, J.J., Ankudinov, A., Albers, R.C., Eller, M.J.: Multiple-scattering calculations of X-ray-absorption spectra. Phys. Rev. B **52**, 2995–3009 (1995)
29. Rehr, J.J., Kas, J.J., Prange, M.P., Sorini, A.P., Takimoto, Y., Vila, F.: Ab initio theory and calculations of X-ray spectra. C. R. Phys. **10**, 548–559 (2009)
30. Rehr, J.J., Kas, J.J., Vila, F.D., Prange, M.P., Jorissen, K.: Parameter-free calculations of X-ray spectra with FEFF9. Phys. Chem. Chem. Phys. **12**, 5503–5513 (2010)
31. Crozier, E.D., Rehr, J.J., Ingalls, R.: Amorphous and liquid systems. In: Koningsberger, D.C., Prins, R. (eds.) X-ray Absorption: Principles, Applications, Techniques of EXAFS, SEXAFS and XANES. Wiley-Interscience, New York (1988)
32. Sundvall, B.: Crystal structure of tetraoxotetrahydroxohexabismuth(III) perchlorate heptahydrate, $Bi_6O_4(OH)_4(ClO_4)_6{\cdot}7H_2O$: an X-ray and neutron diffraction study. Inorg. Chem. **22**, 1906–1912 (1983)
33. Joly, Y.: X-ray absorption near-edge structure calculations beyond the muffin-tin approximation. Phys. Rev. B **63**, 125120 (2001)
34. Testemale, D., Brugger, J., Liu, W.H., Etschmann, B., Hazemann, J.L.: In-situ X-ray absorption study of iron(II) speciation in brines up to supercritical conditions. Chem. Geol. **264**, 295–310 (2009)
35. Fray, S.M., Milne, C.J., Lightfoot, P.: Synthesis and structure of $CaBiO_2Cl$ and $SrBiO_2Cl$. J. Solid State Chem. **128**, 115–120 (1997)
36. Testemale, D., Hazemann, J.L., Pokrovski, G.S., Joly, Y., Roux, J., Argoud, R., Geaymond, O.: Structural and electronic evolution of the $As(OH)_3$ molecule in high temperature aqueous solutions: an X-ray absorption investigation. J. Chem. Phys. **121**, 8973–8982 (2004)
37. Joly, Y., Cabaret, D., Renevier, H., Natoli, C.R.: Electron population analysis by full-potential X-ray absorption simulations. Phys. Rev. Lett. **82**, 2398–2401 (1999)
38. Krause, M.O., Oliver, J.H.: Natural widths of atomic K and L levels, K alpha X-ray lines and several KLL Auger lines. J. Phys. Chem. Ref. Data **8**, 329–337 (1979)
39. Gurney, R.W.: Ionic Processes in Solution. McGraw-Hill, New York (1953)
40. Ryzhenko, B.N.: Equilibria in Hydrothermal Solutions (in Russian). Nauka, Moscow (1981)
41. Bryzgalin, O.V., Rafal'skiy, R.P.: Estimation of instability constants for ore-element complexes at elevated temperatures. Geochem. Int. **19**, 839–849 (1982)
42. Helgeson, H., Kirkham, D.H.: Theoretical prediction of the thermodynamic behavior of aqueous electrolytes at high pressures and temperatures: I. Summary of the thermodynamic/electrostatic properties of the solvent. Am. J. Sci. **274**, 1089–1198 (1974)
43. Kolonin, G.R., Laptev, Y.V.: Study of process of dissolution of α-Bi_2O_3 (bismite) and complex-formation of bismuth in hydrothermal solutions (in Russian). Geokhimiya **11**, 1621–1631 (1982)
44. Shannon, R.D.: Revised effective ionic radii and systematic studies of interatomic distances in halides and chalcogenides. Acta Crystallogr. **A32**, 751–767 (1976)
45. Helgeson, H.C.: Thermodynamics of hydrothermal systems at elevated temperatures and pressures. Am. J. Sci. **267**, 729–804 (1969)
46. Bethke, C.M.: Geochemical and Biogeochemical Reaction Modeling, 2nd edn. Cambridge University Press, Cambridge (2008)